

## Strength Analysis for Shrink Fitting System Used for Ceramics Rolls in the Continuous Pickling Line

Nao-Aki NODA<sup>1,a</sup>, Hendra<sup>1,b</sup>, Masakazu OOSATO<sup>1,c</sup>, Kenta SUZUMOTO<sup>1,d</sup>,  
Yasushi TAKASE<sup>1,e</sup>, and Wenbin LI<sup>1,f</sup>

<sup>1</sup>Department of Mechanical Engineering, Kyushu Institute of Technology, Sensui-cho, Tobata-ku, Kitakyushu-shi, Fukuoka, 804-8550 Japan

<sup>a</sup>noda@mech.kyutech.ac.jp, <sup>b</sup>mpe2\_boy@yahoo.com, <sup>c</sup>h344108m@tobata.isc.kyutech.ac.jp,  
<sup>d</sup>e104061k@tobata.isc.kyutech.ac.jp, <sup>e</sup>Takase@mech.kyutech.ac.jp, <sup>f</sup>wenbin-li@hotmail.com

**Keywords:** Contact Problem, Ceramics, Elasticity, Bending, Finite Element Method.

**Abstract.** Cast iron and steel rolls used in the continuous pickling line must be changed frequently because the continuous acid wash equipment induces wear on the roll surface in a short period. The damage portions are usually repaired by using the flame spray coating. Recently, ceramics materials are planned to be introduced to prevent the damage because of their high abrasion and corrosion resistances. In this study new roll structure is considered where a ceramics sleeve is connected with steel shafts at both ends by shrink fitting. Here, the ceramics sleeve may provide a longer lifetime and reduces the cost for the maintenance. However, attention should be paid to the maximum tensile stresses appearing between the ceramics sleeve, spacer rings and steel shafts because the fracture toughness, plasticity and fatigue strengths of ceramics are extremely lower than the values of steel. In this study, finite element method analysis is applied to the new structure, and the maximum tensile stress and stress amplitude have been investigated with varying the dimensions of the structure. Fatigue strengths of ceramics are also considered under several geometrical conditions.

### Introduction

Pickling is the process of chemically removing oxides and scale from the surface of a metal by the action of water solutions of inorganic acids. Considerable variation in type of pickling solution, operation and equipment is found in the industry. Among the types of pickling equipment may be mentioned the batch picklers, modified batch, non-or semi-continuous and continuous picklers [1]. Fig. 1 shows the schematic diagram of pickling line. As shown in Fig. 1 the continuous acid wash makes the coil surface beautiful by going through hydrochloric acid tank and removing surface scale formed in the previous process. Similar lines for Fig. 1 may be found in coil painting equipment,

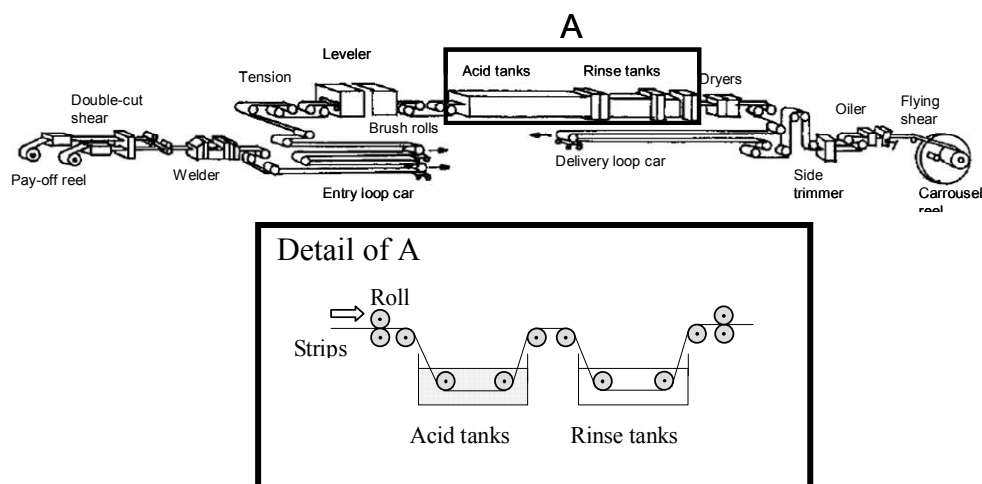


Fig.1 Schematic diagram of new pickling line

which continuously paints the cold rolling lamina coil, galvanizing steel board coil, and aluminum coil, etc. A lot of large rolls are used for those equipments. Currently cast iron, carbon steel, and alloy steel are used as roll materials in the coil painting and also continuous acid wash equipments, which induce wear on the roll surface in a short period. Therefore, the production lines have to be stopped to exchange the rolls requiring a lot of time for maintenance. Then, the damage portions have to be repaired by using the flame spray coating [2].

Fig. 2 shows the structure of the rolls. In this study, we will focus on the roll structure where a sleeve and two short shafts are initially connected by shrink fitting at both ends, and shaft and spacer rings are finally connected by welding as shown in Fig.2. The use of ceramics and cemented carbide is recently promoted [3] because they provide high temperature resistance, high abrasion resistance and anti-oxidation. Here, we consider ceramics sleeve and ceramics spacer rings connected by shrink fitting, which are suitable for reducing the cost for maintenance.

However, to design the hollow rolls as shown in Fig. 2, attention should be paid to the maximum tensile stresses and stress amplitude appearing at the edge of the sleeve. In particular, since fracture toughness and fatigue strengths of ceramics are extremely smaller, stress analysis for the roll becomes more and more important compared with the cases for steel rolls. Therefore, in this study FEM analysis will be applied to the structure as shown in Fig.3, and suitable dimensions will be discussed.

### Analytical Conditions

Define the shrink fitting ratio as  $\delta/d$ , where  $\delta$  is the diameter difference with the diameter  $d$ . Assume that the roll is subjected to distributed load  $w=100\text{N/mm}$  and simply supported at both ends (see Fig.2). The friction coefficient between sleeve and shafts is assumed as 0.3.

Table 1 shows the material properties of ceramics, steel, and cemented carbide. Stainless steel is usually used for rolls but ceramics and cemented carbide rolls may provide a longer maintenance span due to their high corrosion resistance and high abrasion resistance. Fig. 3 shows the finite element mesh model of the rolls. The total number of elements is 37020 and the total number of nodes is

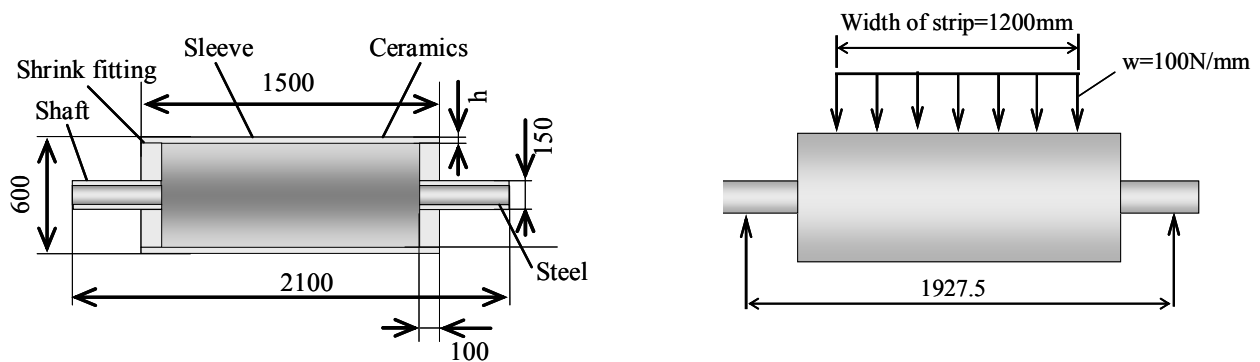


Fig.2 New ceramics roll system (mm)

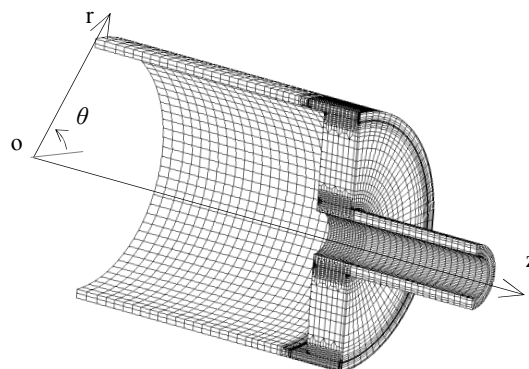
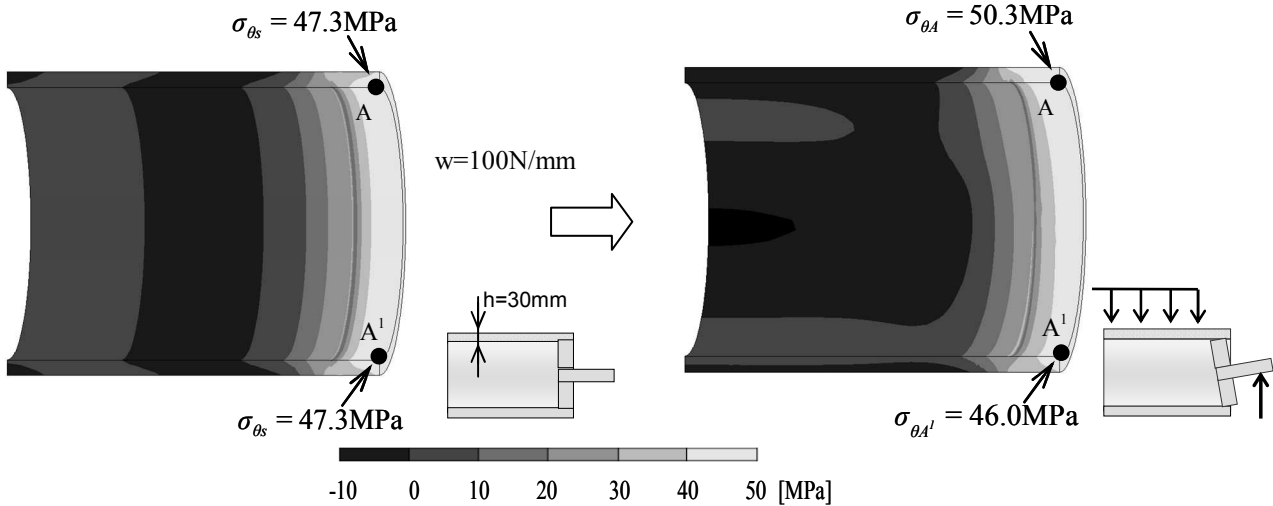


Fig.3 FEM mesh

Table1 Material Properties

	Young's modulus [GPa]	Poisson's ratio	Tensile strength [MPa]	Fracture toughness [MPa√m]	Fatigue strength [MPa]
Ceramics (Si <sub>3</sub> N <sub>4</sub> )	300	0.28	500	7	200
Steel (HV=220)	210	0.3	600	100	300
Cemented Carbide	500	0.24	1000	20	400

26751. The model of 1/4 of the roll is considered due to symmetry.



(a)  $\sigma_\theta$  due to shrink fitting (b)  $\sigma_\theta$  due to shrink fitting and load distribution

Fig.4 Stress distribution  $\sigma_\theta$  when  $\delta/d=1.5 \times 10^{-4}$

**Maximum Tensile Stress Analysis**

**Maximum Tensile Stress.** In this study the range  $\delta/d \leq 1.5 \times 10^{-4}$  is considered because large values  $\delta/d$  are not suitable for ceramics. Fig. 4 shows stress distribution  $\sigma_\theta$  at the shrink fitting ratio  $\delta/d=1.5 \times 10^{-4}$  and the sleeve thickness  $h=30\text{mm}$ . Fig. 4(a) shows the stress  $\sigma_{\theta_s}$  due to shrink fitting and Fig.4 (b) shows maximum stress distribution  $\sigma_{\theta_{max}} (= \sigma_{\theta_s} + \sigma_{\theta_b})$  due to load distribution  $w=100\text{N/mm}$  after shrink fitting. As shown in Fig. 4 (a), the maximum tensile stress at point A and A' are  $\sigma_{\theta_s} = 47.3\text{MPa}$  while shrink fitting. It becomes  $\sigma_{\theta_{max}} = 50.3\text{MPa}$  by applying the distribution load after shrink fitting at point A and  $\sigma_{\theta_{max}} = 46.0\text{MPa}$  at point A' as shown in Fig. 4 (b). In other words,  $\sigma_{\theta_b}$  increases by  $\sigma_{\theta_b} = 2.9\text{MPa}$  at point A.

It is found that the maximum tensile stress appears at point A as  $\sigma_\theta$ . In this chapter we will focus on reducing the maximum tensile stress  $\sigma_\theta$  at A with varying geometrical conditions.

**Effect of Shrink Fitting Ratio  $\delta/d$  and Bending Moment upon the Maximum Tensile Stress.**

Fig. 5 illustrates effects of shrink fitting ratio  $\delta/d$  upon the stresses  $\sigma_{\theta_s}$ ,  $\sigma_{\theta_{max}}$  and  $\sigma_{\theta_b}$ . Fig. 5 (a) shows the stress  $\sigma_{\theta_s}$  vs.  $\delta/d$  and  $\sigma_{\theta_{max}} (= \sigma_{\theta_s} + \sigma_{\theta_b})$  vs.  $\delta/d$  relationships when the load distribution  $w=100\text{N/mm}$  is applied after shrink fitting when  $h=20\text{mm}$ . From Fig.5 (a), it is found that  $\sigma_{\theta_s}$  increases with increasing  $\delta/d$  and  $\sigma_{\theta_{max}}$  has a minimum value at  $\delta/d=1.5 \times 10^{-4}$ . On the other hand,  $\sigma_{\theta_b}$  decreases with increasing  $\delta/d$  as shown in Fig. 5 (b). From Fig.5 (b), it is found that the

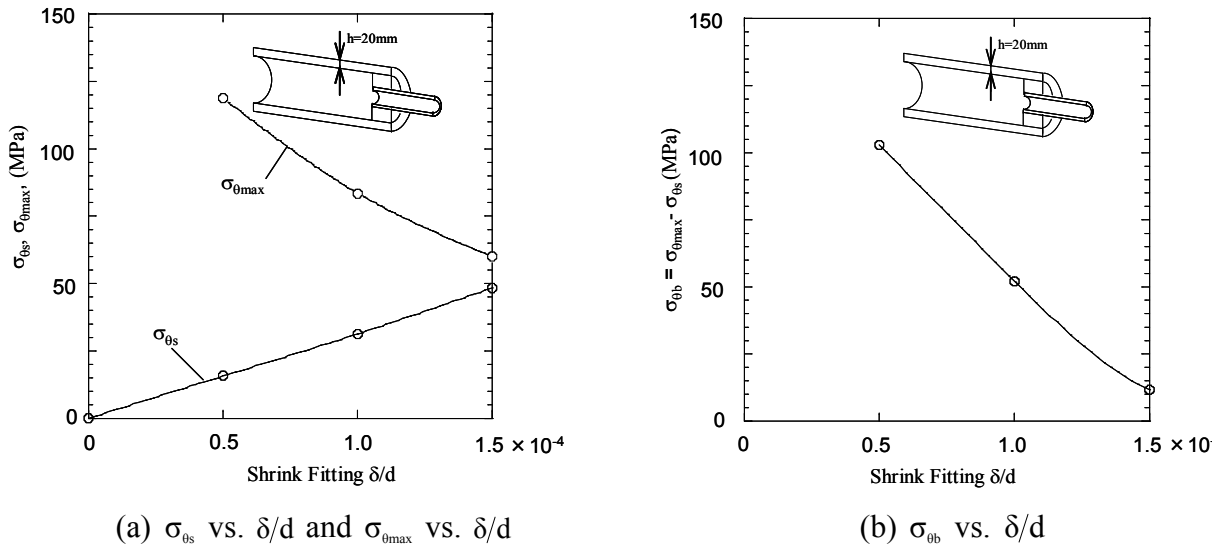


Fig.5  $\sigma_{\theta}$  vs.  $\delta/d$  when  $h=20\text{mm}$

( $\sigma_{\theta_{max}} (= \sigma_{\theta_s} + \sigma_{\theta_b})$ ,  $\sigma_{\theta_s}$  : Stress due to shrink fitting,  $\sigma_{\theta_b}$  : Stress due to load distribution)

large  $\delta/d$  reduces the contact stress  $\sigma_{\theta_b}$  by gripping the shaft tightly. It may be concluded that  $\sigma_{\theta_{max}} (= \sigma_{\theta_s} + \sigma_{\theta_b})$  may decrease with increasing  $\delta/d$ .

**The Effect of Thickness  $h$  on  $\sigma_{\theta_b}$ .** Fig. 6 shows  $\sigma_{\theta_s}$  vs.  $\delta/d$  and  $\sigma_{\theta_b} = \sigma_{\theta_{max}} - \sigma_{\theta_s}$  vs.  $\delta/d$  relations when the load distribution  $w=100\text{N/mm}$  is applied after shrink fitting for different thickness  $h$ . Here, we assume three different thicknesses,  $h=10\text{mm}$ ,  $h=20\text{mm}$ , and  $h=30\text{mm}$ . From Fig.6 (a), it is seen that  $\sigma_{\theta_s}$  increases with increasing  $\delta/d$ . It should be noted that  $\sigma_{\theta_s}$  decreases with increasing the sleeve thickness  $h$ . Similarly,  $\sigma_{\theta_b}$  decreases with increasing sleeve thickness  $h$  in Fig. 6 (b). When the  $\delta/d$  is larger, the spacer rings and sleeve can be treated as a unit body bonded perfectly.

**Fatigue Strengths Analysis of Ceramics Rolls**

Maximum stresses are found to be lower than the tensile stress 500MPa as shown in the previous chapter. However, fatigue strengths should be also considered for ceramics. Fig. 7 (a) indicates the

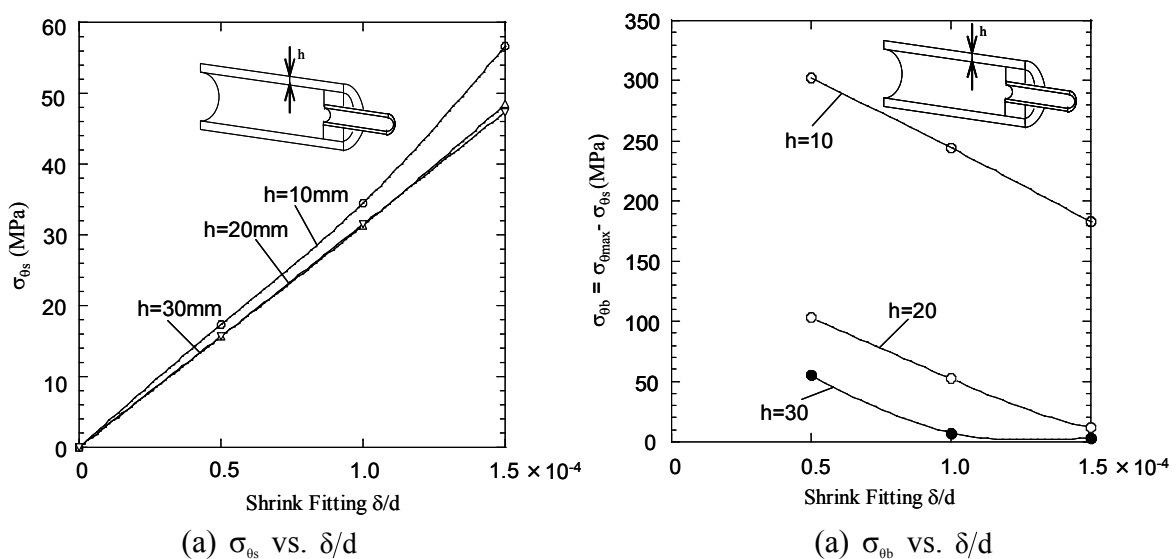
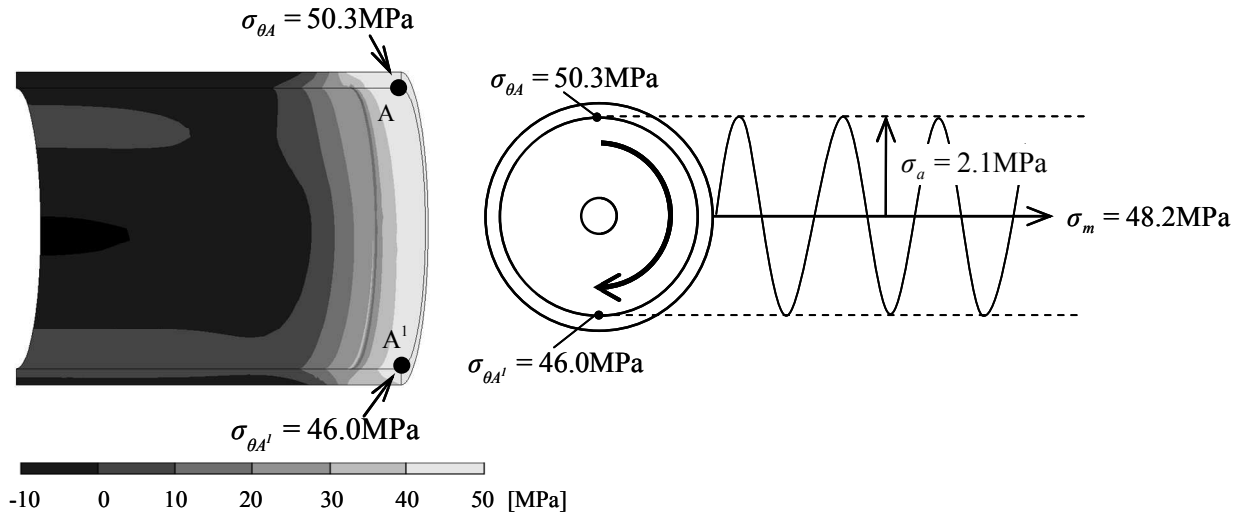
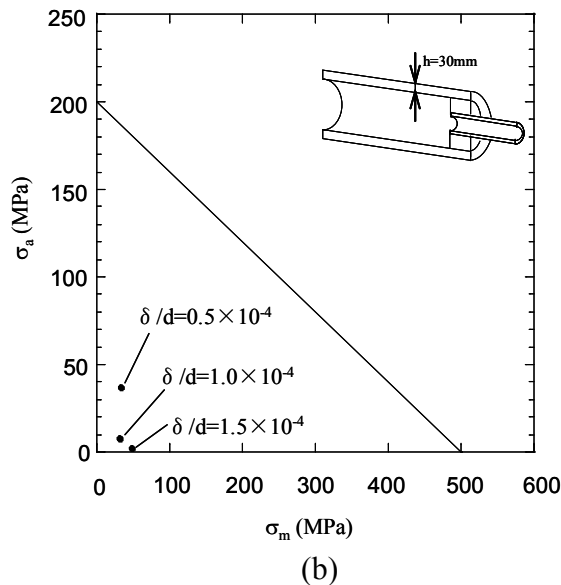


Fig.6  $\sigma_{\theta}$  vs.  $\delta/d$  when  $h=10, 20,$  and  $30\text{mm}$

( $\sigma_{\theta_s}$  : Stress due to shrink fitting,  $\sigma_{\theta_b}$  : Stress due to load distribution)



(a)  $\sigma_{\theta}$  due to shrink fitting and load distribution



(b) Fig. 7 Mean stress and stress amplitude for ceramics

mean stress  $\sigma_m = (\sigma_{\theta A} + \sigma_{\theta A'})/2$  and stress amplitude  $\sigma_a = (\sigma_{\theta A} - \sigma_{\theta A'})/2$  at shrink fitting ratio  $\delta/d = 1.5 \times 10^{-4}$  when thickness  $h = 30 \text{ mm}$ . Due to the rotation of rolls, the largest value of  $\sigma_{\theta}$  varies from 50.3 MPa to 46.0 MPa as shown in Fig. 7 (a). Then, the corresponding value of mean stress  $\sigma_m = 48.2 \text{ MPa}$  with the value of stress amplitude  $\sigma_a = 2.1 \text{ MPa}$ . With increasing the shrink fitting ratio  $\delta/d$ , the mean stress increases but the stress amplitude decreases. As shown in Fig. 7 (b), it is found that the values of stress amplitude  $\sigma_a$  and mean stress  $\sigma_m$  are below the fatigue strengths of ceramics material.

## Conclusions

Cast iron and steel rolls used in the continuous pickling line must be changed frequently because the continuous acid wash equipment process induces wear on the roll surface in a short period. Therefore the production lines have to be stopped to exchange the rolls with requiring a lot of time for maintenance. To reduce maintenance cost for exchanging the rolls, in this study, a new structure was considered where a ceramics sleeve connected with ceramics spacer rings and steel shafts at both ends

by shrink fitting. Strengths analysis was performed with the application of the finite element method with varying several geometrical conditions. The conclusions can be made in the following way.

1. The maximum tensile stress is appearing at the end of the sleeve as  $\sigma_{\theta_{\max}}$ . The stress  $\sigma_{\theta_{\max}}$  may be expressed as  $\sigma_{\theta_{\max}} (= \sigma_{\theta_s} + \sigma_{\theta_b})$  where  $\sigma_{\theta_s}$  is a shrink fitting stress and  $\sigma_{\theta_b}$  is a stress due to load distribution. For example, the maximum tensile stress at point A and A<sup>1</sup> are  $\sigma_{\theta_s} = 47.3\text{MPa}$  while shrink fitting when the thickness  $h=30\text{mm}$ , shrink fitting ratio  $\delta/d=1.5 \times 10^{-4}$ . It becomes  $\sigma_{\theta_{\max}} = 50.3\text{MPa}$  by applying the distribution load after shrink fitting at point A and  $\sigma_{\theta_{\max}} = 46.0\text{MPa}$  at point A<sup>1</sup>. In other words,  $\sigma_{\theta_b}$  increases by  $\sigma_{\theta_b} = 2.9\text{MPa}$  at point A.
2. For small values of  $\delta/d$ , the maximum stress  $\sigma_{\theta_{\max}}$  becomes larger because large contact stresses may appear between the sleeve and shafts, especially for small thickness. The values of  $\delta/d=1.5 \times 10^{-4}$  may reduce  $\sigma_{\theta_{\max}}$  effectively. In other words,  $\sigma_{\theta_{\max}}$  takes a minimum value at  $\delta/d=1.5 \times 10^{-4}$ .
3. The effect of thickness of the sleeve was considered. It is seen that  $\sigma_{\theta_s}$  increases with increasing  $\delta/d$ . It should be noted that  $\sigma_{\theta_s}$  decreases with increasing the sleeve thickness  $h$ . Similarly,  $\sigma_{\theta_b}$  decreases with increasing sleeve thickness  $h$  in Fig. 6 (b).
4. Fatigue strength was also considered for ceramics rolls. When  $\delta/d=1.5 \times 10^{-4}$  with thickness  $h=30\text{mm}$ , it is found that the values of stress amplitude  $\sigma_a$  and mean stress  $\sigma_m$  are below the fatigue strengths of ceramics material.

## References

- [1] US Patent 5412966, *Push-pull pickle line*, Available from <[www.freepatentsonline.com](http://www.freepatentsonline.com)>.
- [2] E. Miki : Plant Engineer Vol.21, No.1, (1989), pp.8-12 (in Japanese).
- [3] T. Iwata, and H. Mori: Plant Engineer Vol.15, No.6, (1983), pp.55-59 (in Japanese).
- [4] S. Harada, N. Noda, O. Uehara, and M. Nagano: Transactions of the Japan Society of Mechanical Engineering Vol.57, No.539, (1991), pp.173-178.
- [5] M. Tsuyunaru, N. Noda, A. Hendra and Y. Takase: Transactions of the Japan Society of Mechanical Engineering Vol.74, No.743, (2008), pp.919-925 (in Japanese).

## **Fracture and Strength of Solids VII**

doi:10.4028/www.scientific.net/KEM.462-463

## **Strength Analysis for Shrink Fitting System Used for Ceramics Rolls in the Continuous Pickling Line**

doi:10.4028/www.scientific.net/KEM.462-463.1140